applied sciences

MDPI

Article

A Simplistic Downlink Channel Estimation Method for NB-IoT

Jarosław Magiera

Faculty of Electronics, Telecommunications and Informatics, Gdańsk University of Technology, ul. G. Narutowicza 11/12, 80-233 Gdańsk, Poland; jaroslaw.magiera@pg.edu.pl

Abstract: This paper presents a downlink channel estimation method intended for a Narrowband Internet of Things (NB-IoT) access link. Due to its low computational complexity, this method is well suited for energy-efficient IoT devices, still providing acceptable reception quality in terms of signal-to-noise (SNR) performance. This paper describes the physical layer of NB-IoT within the scope of channel estimation, and also reviews existing channel estimation methods for OFDM signals. The proposed method, based on linear interpolation of channel coefficients, is described as a three-step procedure. Next, indicators of channel quality assessment, which may be determined without prior knowledge about the transmitted signal, are defined. Two variants of channel estimation, differing in the frequency domain processing, are evaluated to assess the significance of frequency selectivity in an NB-IoT downlink. The chosen method is compared with another method implemented in MATLAB LTE Toolbox™. An analysis of the computation time is conducted, subsequently demonstrating the definite advantage of the proposed method.

Keywords: downlink channel estimation; NB-IoT; Internet of Things; LPWAN; M2M communications; physical layer

Citation: Magiera, J. A Simplistic Downlink Channel Estimation Method for NB-IoT. *Appl. Sci.* **2023**, *13*, 12615. https://doi.org/10.3390/app132312615

Academic Editor: Gianluigi Ferrari

Received: 18 October 2023
Revised: 14 November 2023
Accepted: 20 November 2023
Published: 23 November 2023

1. Introduction

Narrowband Internet of Things (NB-IoT) is a low-power wide-area network (LPWAN) technology designed to enable efficient machine-to-machine (M2M) communication. It emerged from the LTE technology as LTE-NB1 and LTE-NB2 standards, introduced in 3GPP specifications Release 13 and 14, respectively, [1,2]. It is assumed that NB-IoT user equipment (UE) will operate for several years without battery replacement. Thus, NB-IoT devices require a special design to maintain low-power consumption. This refers not only to optimal hardware implementation, but also to the development of efficient and low-complexity physical layer processing algorithms. It is especially important to optimize downlink procedures, as receive algorithms are generally more complex than transmit ones. Well-designed algorithms should be kept simple, still providing acceptable receive quality in challenging propagation conditions. IoT devices are likely to be installed in locations with a low signal-to-noise ratio (SNR), like basements, underground facilities, factory sites, etc. [3].

One of the fundamental procedures of downlink signal processing is channel estimation, which provides information about the distortion of the received signal, caused mainly by multipath fading, carrier frequency offset and phase noise [4–7]. This information is further utilized in the channel equalization step, which compensates for channel impairments to provide phase-amplitude alignment of a complex constellation for further demodulation and decoding. To make channel estimation possible, the transmitted signals contain reference elements (pilots) which are known to the receiver. Channel distortion of these elements may be estimated and extended to other components of the received signal.

1.1. Channel Estimation in NB-IoT Downlink

Similar to LTE, the NB-IoT downlink physical layer is based on the OFDM transmission scheme [8]. A reference signal is transmitted in resource elements at specific subcarriers

and symbols. The NB-IoT physical layer, designed to allow for coexistence with LTE transmissions, uses a single physical resource block (PRB) of 180 kHz [9]. For downlink transmission, 12 OFDM subcarriers are available, separated by 15 kHz. In the time domain, the downlink is organized into 10 ms frames. Each frame consists of 10 subframes divided into 2 slots, each carrying 7 OFDM symbols [10,11]. A dedicated reference signal, called Narrowband Reference Signal (NRS), is introduced in the NB-IoT downlink. NRS is a pseudorandom sequence of complex numbers mapped onto QPSK constellation points. Real and imaginary parts of these numbers correspond to even and odd elements of a $2^{31} - 1$-bit long Gold sequence. An NRS is assigned four resource elements located in the last two symbols of each NB-IoT subframe slot. If the eNodeB (eNB) base station uses two antenna ports for NB-IoT transmit diversity, each of these ports is assigned an NRS with a different resource allocation. The four NRS subcarrier indices are dependent on the NB-IoT cell identifier (NB cell ID) according to [12]. An NRS is not transmitted in subframes reserved for synchronization signals (NPSS and NSSS). Figure 1 presents the possible allocation of NRS resources in a single subframe.

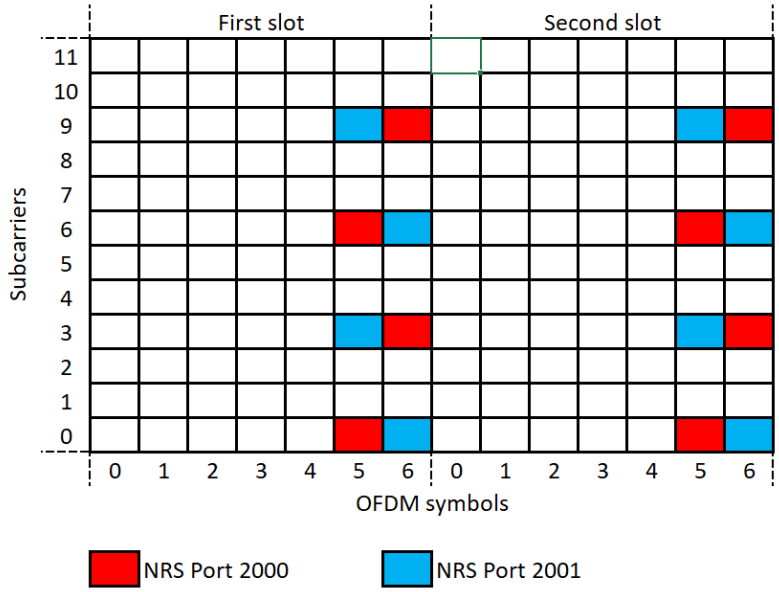

Figure 1. Example of resource allocation for NRS in single NB-IoT downlink subframe.

The role of NRS is to provide reference elements (pilots) whose original values are known at the receiver side. The channel estimation starts by estimating channel coefficients for pilots. Next, the channel response is populated for the entire time-frequency resource grid within a designated time window. The following subsection briefly reviews the channel estimation methods proposed in the literature.

1.2. Related Work

The procedure of channel estimation is not standardized, thus it is up to a UE designer to implement an algorithm with an appropriate balance between SNR performance and complexity [13]. Many solutions proposed in the literature are based on Least Squares (LS) or Minimum Mean Square Error (MMSE) algorithms which were originally intended for wireless OFDM links in general [14,15]. MMSE is not preferable for NB-IoT, as it requires matrix inversion which results in higher complexity, although some modifications were proposed to reduce it [16]. The Maximum Likelihood (ML) approach is known to be optimal in terms of SNR performance, yet it is the most computationally intensive [17]. LS and Linear MMSE (LMMSE) algorithms were further adapted for the LTE radio interface [18–22]. However, the power consumption requirements on wideband LTE UEs are not so stringent as for NB-IoT devices. In recent years, several channel estimation methods for NB-IoT were

presented. In [23], the authors propose a sequential method based on an MMSE estimator. A modified LS approach with random sorting of channel impulse responses is described in [24]. A method using LMMSE with singular value decomposition (SVD) is described in [25,26], while yet another approach, based on ML and a time-domain Wiener filter, is proposed in [27].

1.3. Contributions

In this paper, a channel estimation method is proposed for NB-IoT downlink. The method features a simple approach for populating channel coefficients based on pilot estimates. Sparse NRS pilots are estimated using the conventional LS algorithm. Next, the channel coefficients for all resource elements in a transmission frame are calculated through interpolation in the time (symbol) domain, followed by either interpolation or averaging in the frequency (subcarrier) domain. The two approaches in the frequency domain are compared to evaluate their performance in fading channel conditions. This paper evaluates the SNR performance of the proposed scheme to verify that it does not have a higher level of channel estimation error compared to the method that uses a more complex interpolation scheme. Moreover, the computational complexity was investigated by comparing the processing delays among methods. The main objective of this paper is to determine whether a simplified channel coefficient population scheme has a negative impact on the quality of channel estimation in a narrowband frequency channel designated for NB-IoT downlink.

It is worth noting that this paper presents the results obtained by recording actual NB-IoT signals generated by a professional radio communication tester. This is in contrast to other papers on this topic, which often focus solely on theoretical analysis and software simulation results. Using a hardware testbed requires a modified channel estimation evaluation methodology because the values of the original channel coefficients are not accessible. Two performance indicators are introduced in this paper to evaluate channel estimation. These indicators rely solely on information recovered from received signals.

1.4. Organization of the Paper

The remainder of this paper is organized as follows. Section 2 introduces the proposed channel estimation technique. Section 3 presents evaluation methodology for the assessment of the channel estimation method. Section 4 describes the test setup used to measure the channel quality indicators. Section 5 shows the results of the measurements, including the SNR performance and the computation time. The closing section discusses the outcomes of this study.

2. NB-IoT Channel Estimation Procedure

This section presents the proposed algorithm for downlink channel estimation whose objective is to compute channel coefficients. A channel coefficient, denoted by h, is a complex number whose modulus and argument correspond to the attenuation and phase shift introduced during signal transmission. Each h value refers to an OFDM resource element on a specific subcarrier k of a given symbol n

$$y_{n,k} = h_{n,k} \cdot x_{n,k} + \eta_{n,k}, \tag{1}$$

where x, y and η represent a transmitted resource element, a received resource element and additive interference, respectively.

A set of channel coefficients is calculated per frame, i.e., every 10 ms. The first step is to calculate h values for NRS resource elements only. The LS method is used, according to which the estimate of channel coefficient $\hat{h}$ is calculated as follows [14,20]:

$$\hat{h}^{LS}_{\bar{n},\bar{k}} = x^{-1}_{\bar{n},\bar{k}} \cdot y_{\bar{n},\bar{k}}, \tag{2}$$

where $\{\bar{n}, \bar{k}\}$ pairs address NRS resource elements. The component $x(\bar{n}, \bar{k})$ is known here as it is the element of an NRS sequence. In short, NRS channel coefficients are estimated by complex division of the received NRS resource elements by respective reference NRS resource elements. It is a simple calculation, not requiring matrix inversion, as opposed to the MMSE method.

In the next steps of the algorithm, channel coefficients are estimated for all the OFDM resource elements other than NRS ones. Firstly, time-domain interpolation is performed on NRS subcarriers. In order to keep the calculation complexity low, linear interpolation was chosen. Let $\bar{n}'$ and $\bar{n}''$ be OFDM symbol indices corresponding to subsequent NRS resource elements on subcarrier $\bar{k}$. Channel coefficients for the resources lying between these elements are calculated as follows:

$$\hat{h}_{n,\bar{k}} = \hat{h}_{\bar{n}',\bar{k}} + \frac{n - \bar{n}'}{\bar{n}'' - \bar{n}'} \cdot (\hat{h}_{\bar{n}'',\bar{k}} - \hat{h}_{\bar{n}',\bar{k}}) \qquad n = \bar{n}' + 1, \ldots, \bar{n}'' - 1. \tag{3}$$

Channel coefficients are complex numbers, so the interpolation is performed separately for their moduli and arguments. An additional phase unwrapping step is necessary prior to the actual interpolation. However, with this method, the resulting phase transitions are more smooth than in the case of the interpolation of real/imaginary components.

It should be noted that symbol spacing between consecutive NRS elements varies. In most cases $\bar{n}''$ is offset from $\bar{n}'$ by seven symbols (see Figure 1). However, some subframes do not contain NRS component. This refers to non NB-IoT subframes (e.g., LTE subframes in the in-band operation mode) and synchronization subframes. In such cases, the linear interpolation is performed at adequately longer intervals.

As mentioned before, channel estimation is performed on a per-frame basis. This might cause discontinuities in channel coefficients between consecutive frames. To solve this problem, channel estimation is performed on 147 OFDM symbols, including one full frame (140 symbols) and the first slot of the following frame (7 symbols). Channel coefficients partially determined for this slot are passed to the next iteration of the channel estimation procedure.

Figure 2 presents an example of linear interpolation of NB-IoT channel coefficients on NRS subcarriers for two consecutive frames. The circle markers represent coefficients calculated for NRS symbols using LS. The dot markers represent interpolated coefficients. The larger spacing between the circles corresponds to NPSS and NSSS subframes. As can be seen, the estimation follows the amplitude and phase variations smoothly and continuously. These variations reflect propagation in the channel modelled according to the Extended Pedestrian A profile with the maximum carrier Doppler shift of 5 Hz (EPA 5 Hz), without additive interference.

In the third step of the procedure, channel coefficients for the remaining eight non-NRS subcarriers are determined. Two variants were considered for this purpose. The first one assumes linear interpolation in the frequency domain, similar to the interpolation in the time domain. Only components located between NRS subcarriers would be calculated in this way, whereas for other subcarriers, zero-order hold is applied. For example, if the NRS subcarrier indices are 2, 5, 8 and 11, the channel coefficients for subcarriers 0 and 1 will have the same value as the coefficient calculated for the lowest NRS subcarrier, i.e., the one with index 2.

The second approach is to apply frequency-domain averaging instead of interpolation. In this case, channel coefficients for all the subcarriers are equal, being the mean value of 4 coefficients estimated earlier for NRS subcarriers. This method is less complex than interpolation; however, its SNR performance needs evaluation. Frequency averaging is suitable for channels without inter-symbol interference (ISI), i.e., when the channel magnitude response is flat. To fulfill this requirement in the case of NB-IoT, the multipath delay spread should be shorter than the reciprocal of 180 kHz frequency bandwidth, i.e., 5.6 µs. In 3GPP multipath propagation models for LTE access link, such as extended

typical urban (ETU), extended vehicular A (EVA) or EPA, the delay spread does not exceed 5 µs [28,29]. It is therefore expected that the averaging approach can be applied successfully.

Once the channel coefficients are estimated for the whole frame, they are passed on to the channel equalization block which compensates for the amplitude and phase distortions of particular resource elements. If transmit diversity is used for downlink transmission, channel equalization is joint with space-frequency block decoding [30].

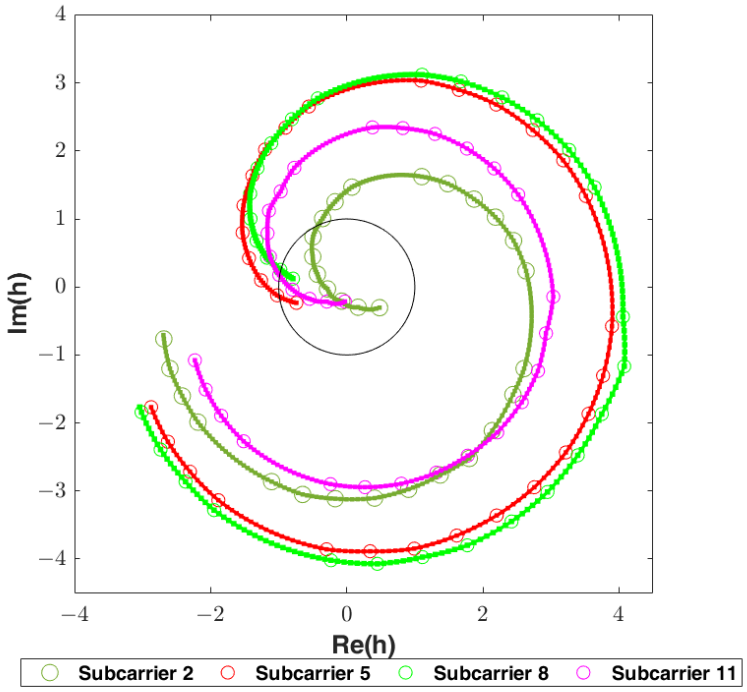

Figure 2. Interpolated channel coefficients on NRS subcarriers (EPA channel profile).

3. Evaluation Methodology

In order to assess the performance of the proposed channel estimation scheme, appropriate quality indicators are required. Some authors use the bit error rate (BER) vs. SNR curves for this purpose. However, this approach is adequate mainly for simulation research, where bit sequences contained in transport blocks are known a priori and may be compared with sequences at the channel decoder output. In the case of signals originating from an eNB or a radio communication tester, this information is not available. For this reason, proper evaluation of BER in the physical layer is cumbersome as information bits are not recovered independently but as whole transport blocks, the validity of which is determined through cyclic redundancy check (CRC).

In this paper, alternative indicators of channel estimation quality, which may be applied directly on the UE side without any prior knowledge about the transmitted downlink signal, are proposed. The quality assessment is based on the analysis of restored QPSK constellation. The error of symbol recovery is evaluated by comparing the symbols from channel equalization output with their original constellation points, which are restored by reverting the downlink signal processing chain, as shown in Figure 3.

Full downlink physical layer processing is implemented, starting from time-frequency synchronization and OFDM FFT demodulation (not included in Figure 3) to channel decoding and transport block recovery. If the transport block is received correctly, which is verified by CRC check, its bits are again channel encoded and processed further until a set of reference QPSK symbols is obtained with the values from the original QPSK constellation, i.e., $\pm 1 \pm 1i$.

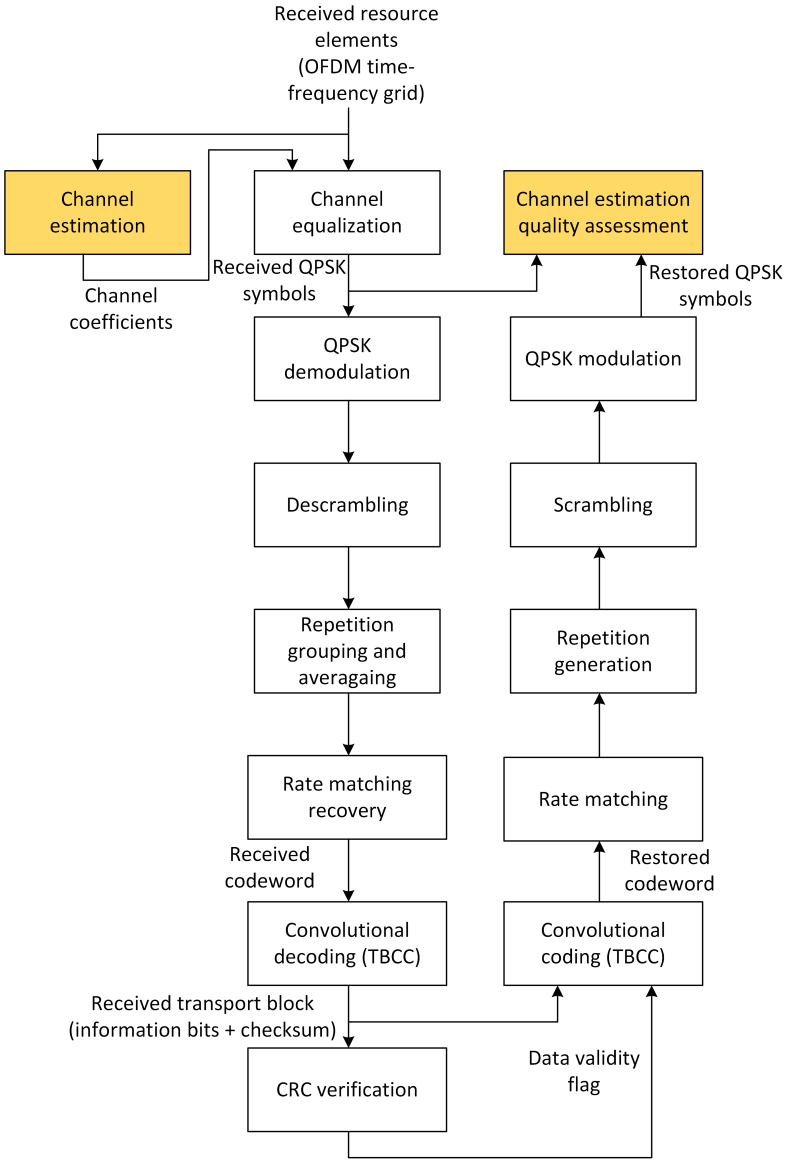

Figure 3. Restoring original QPSK symbols for channel estimation quality assessment.

Two indicators are proposed to evaluate the relation between the received symbols and the restored QPSK symbols. The first one is the root-mean-square error (RMSE) of the symbol phase. It is calculated as follows:

$$\Delta\theta_{RMS} = \sqrt{\frac{1}{N_{symb}} \sum_{i=1}^{N_{symb}} (\theta_i - \theta_{i,ref})^2} \ [rad], \tag{4}$$

where θ represents the symbol phase and N_{symb} is the number of the analyzed complex symbols.

However, evaluating only the phase error may not be sufficient for implementations which make use of soft convolutional decoding, where symbol amplitudes affect path metric values in maximum likelihood sequence estimation (MLSE). Thus, a more comprehensive measure is proposed, namely the symbol correlation coefficient, which combines the impacts of phase and amplitude errors. It is calculated as follows:

$$\rho_{IQ} = \frac{1}{\alpha} \cdot \sum_{i=1}^{N_{symb}} (I_i \cdot I_{i,ref} + Q_i \cdot Q_{i,ref}), \tag{5}$$

where α is the normalization coefficient which limits the ρ_{IQ} values to the range between -1 and 1:

$$\alpha = \sum_{i=1}^{N_{symb}} (|I_i| + |Q_i|). \tag{6}$$

Normally the ρ_{IQ} ranges between 0 and 1. The higher value reflects more accurate symbol reception, whereas negative values would indicate the rotation between the received and reference symbol constellation. To provide a view on the relationship between ρ_{IQ} and the accuracy of the received symbols, a few example constellation graphs are presented in Figure 4. For lower cases, some symbol points are not visible on the graph due to axes limitations introduced to keep equal scales of all the subplots. These graphs were obtained for the proposed channel estimation method, in the additive white Gaussian noise (AWGN) channel at SNR values of -5 dB, 0 dB, 5 dB, and 10 dB, respectively.

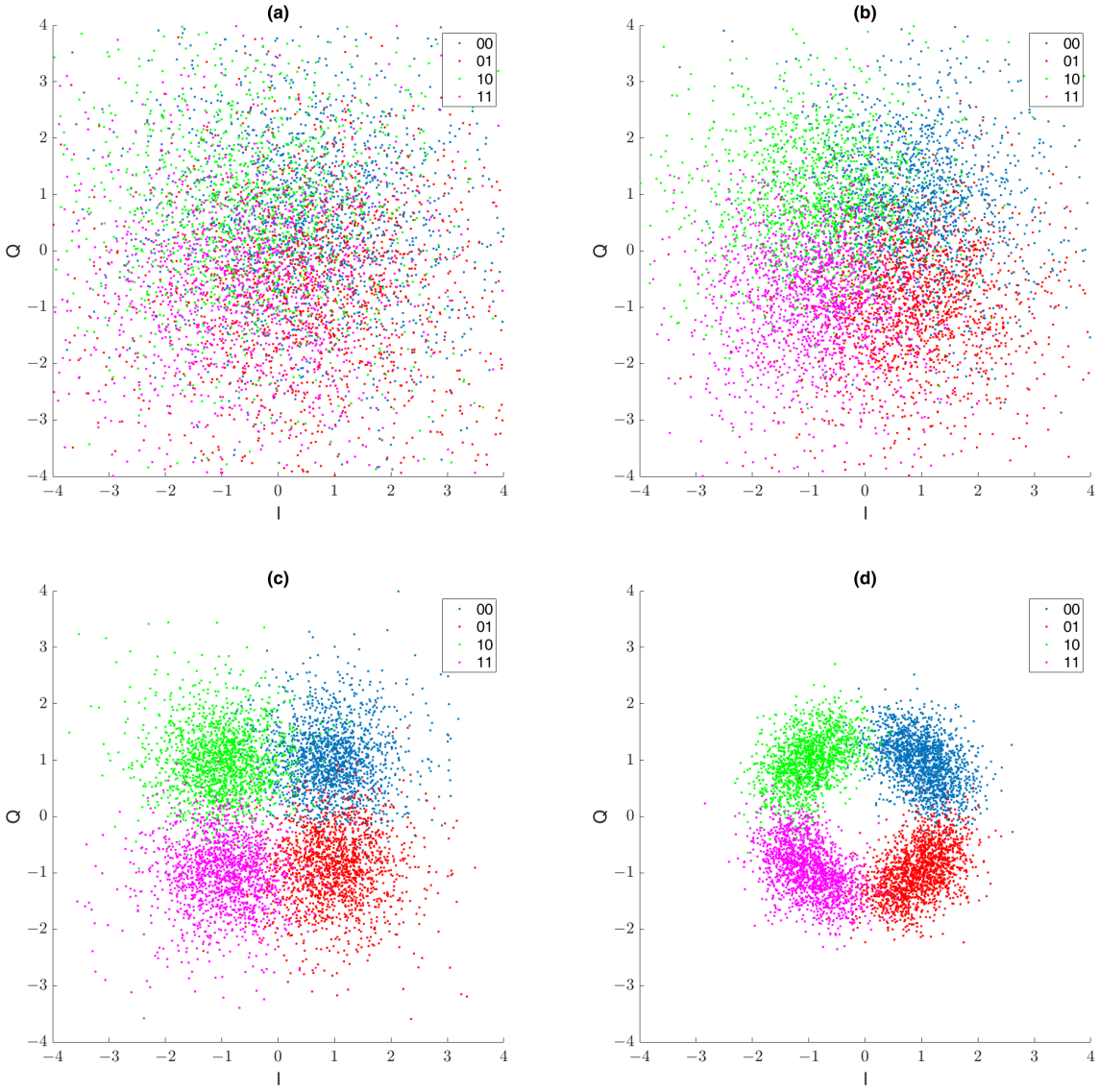

Figure 4. Received symbols represented as points on IQ plane for different values of symbol accuracy coefficient: (**a**) ρ_{IQ} = 0.45, (**b**) ρ_{IQ} = 0.809, (**c**) ρ_{IQ} = 0.966, (**d**) ρ_{IQ} = 0.993.

4. Measurement Setup

To evaluate the performance of the proposed channel estimation method, a series of test waveforms were captured and processed. An R&S® CMW500 radio communication tester [31] was used as an NB-IoT downlink signal source, as shown in Figure 5. Test signals were generated for 2 channel types: AWGN (without multipath fading) and EPA 5 Hz (EPA multipath profile with 5Hz maximum Doppler shift). For both channel types, 4 SNR values were considered: −5 dB, 0 dB, 5 dB and 10 dB. The radio tester was connected to the Ettus Research USRP X310 software defined radio platform, which was used to capture the waveforms of the test signals. For every [channel type, SNR] pair, a series of waveforms was recorded. They were further passed through a dedicated software-defined NB-IoT UE receive path developed in MATLAB environment.

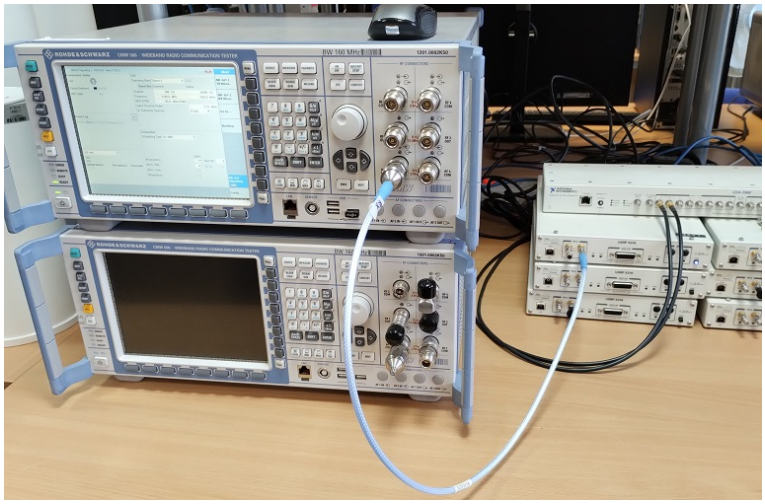

Figure 5. The test bed for generating NB-IoT downlink signals and capturing waveforms.

The algorithm for processing waveform files is shown in Figure 6. Each iteration starts with the frequency and time synchronization step which also provides information about NB cell ID and frame number modulo 8. The synchronization is considered successful if the decoded NB cell ID matches the one set in the tester and the absolute frequency shift does not exceed 1 kHz. Once the waveform is properly aligned in time and frequency, further processing steps are conducted, with a view to decode the Master Information Block (MIB-NB) whose transmission is repeated every 64 frames. If MIB-NB reception is successful, i.e., CRC verification is passed, the block is decoded in order to extract the information necessary to retrieve the subsequent System Information Block Type 1 (SIB1-NB). Receiving SIB1-NB requires processing 256 consecutive frames. If MIB-NB and SIB1-NB are both decoded successfully, bits of their transport blocks are used to calculate channel estimation quality indicators, according to the procedure shown in Figure 3.

The waveform processing loop proceeds to the next iteration either after successful decoding of SIB1-NB or in the case of synchronization/decoding failure. In each iteration, waveform processing starts from the sample which is offset by 640 ms in relation to the previous iteration. Such time shift corresponds to the transmission time interval (TTI) of MIB-NB (64 frames × 10 ms) [32] which ensures that a different MIB-NB is processed at every iteration. In other words, each iteration is an independent trial of synchronization followed by MIB/SIB1 decoding. The success rate of the latter may be considered an additional, higher-level measure of channel estimation quality. The better the channel estimation is, the fewer failures of MIB/SIB1 reception should occur.

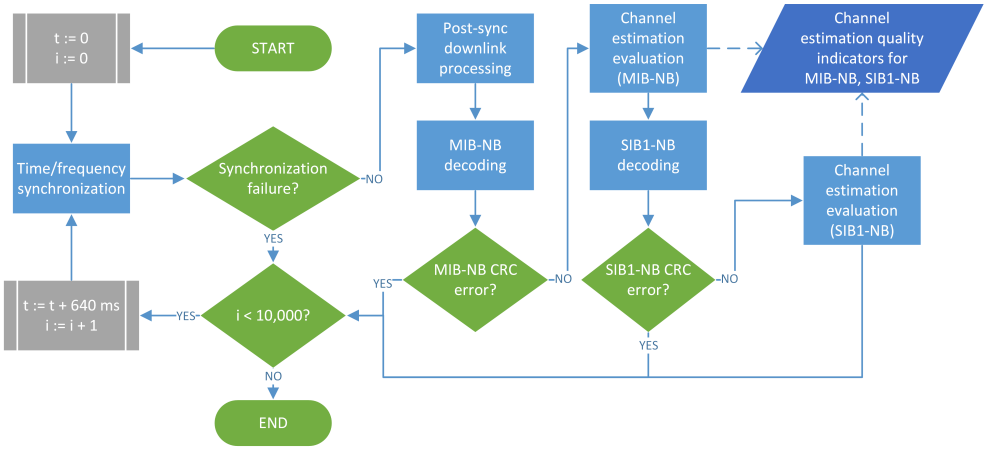

Figure 6. Algorithm for processing a file with captured NB-IoT waveform.

5. Measurement Results

The captured waveforms were processed one after another according to the algorithm shown in Figure 6. For each waveform file, 10,000 iterations were conducted, which required the record duration to be approximately 2 h 47 min (over 6400 s). First, the synchronization success rate was evaluated for each [channel type, SNR] pair. The results are presented in Table 1. As may be seen, the synchronization procedure performs better in the AWGN channel, while in the fading channel it is strongly related to SNR level. Nevertheless, in each case at least 9000 iterations were successful, which is sufficient for the evaluation of channel estimation.

Table 1. Percentage of successful time-frequency synchronizations.

SNR	AWGN Channel	EPA 5 Hz Channel
−5 dB	99.4%	90.1%
0 dB	100.0%	93.9%
5 dB	100.0%	98.3%
10 dB	100.0%	99.2%

5.1. Interpolation vs. Averaging in the Frequency Domain

As mentioned in Section 2, two approaches are considered for populating channel coefficients, namely time interpolation with frequency interpolation (TIFI) and time interpolation with frequency averaging (TIFA). The latter is preferred due to lower computational complexity. However, its SNR performance needs to be evaluated in the fading channel scenario, where channel response is not as flat as in the case of AWGN.

Channel estimation performance indicators were evaluated for both approaches, and the results are presented in Figures 7 and 8. As can be seen, frequency averaging, despite providing only one coefficient per OFDM symbol, performs better for both AWGN and EPA channel profiles. The improvement is particularly noticeable for low SNR conditions in the AWGN channel where TIFA demonstrates significantly lower phase RMSE and a higher symbol correlation coefficient. In the fading channel, TIFA performs better in terms of phase SNR. The performance expressed by symbol correlation is similar for TIFI and TIFA.

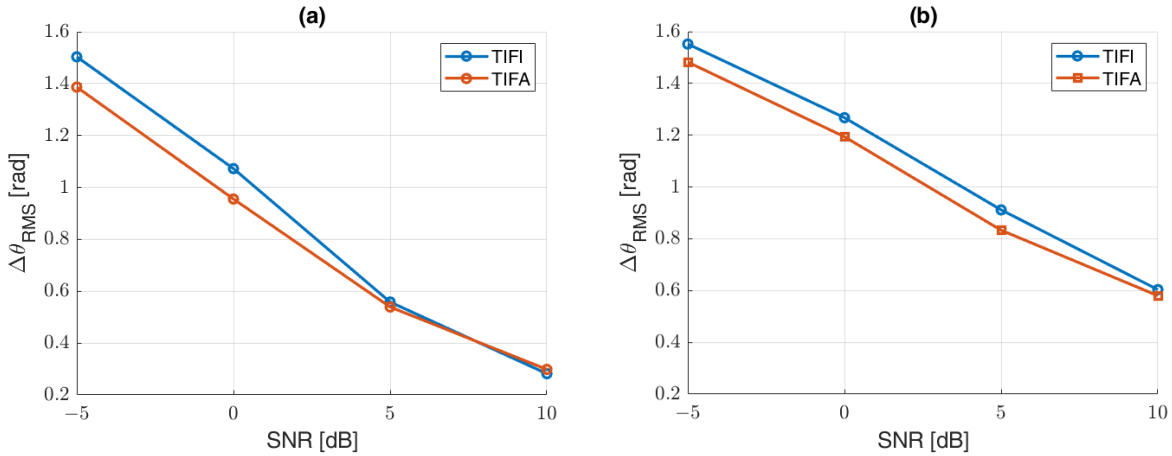

Figure 7. Phase RMS error for (**a**) AWGN channel, (**b**) fading channel (EPA 5 Hz).

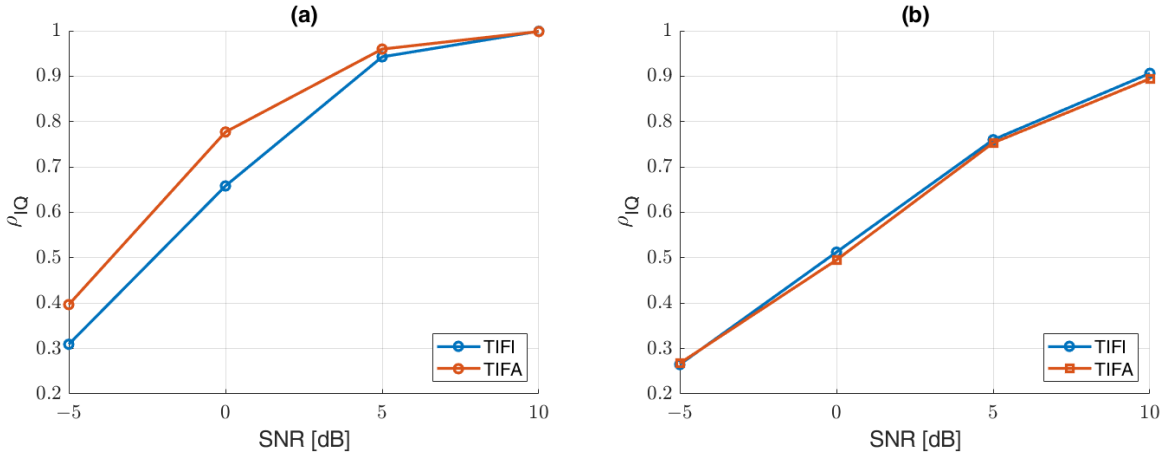

Figure 8. Symbol correlation coefficient for (**a**) AWGN channel, (**b**) fading channel (EPA 5 Hz).

5.2. Comparison of SNR Performance with the Existing Method

Once it was verified that the frequency averaging approach presents acceptable performance, TIFA was compared with the channel estimation method implemented in MATLAB R2020b LTE Toolbox™ (MLT). To be precise, the *lteDLChannelEstimate* function is used to estimate the channel response. According to the documentation, this function implements the method described in 3GPP TS 36.104/TS 36.141 Annex E/F for the purposes of transmitter EVM testing for LTE downlink. However, the above method is intended for LTE, assuming the usage of multiple adjacent PRBs. For an NB-IoT case [33], the function provides a different processing scheme, consisting of three stages: least squares pilot estimation, pilot averaging and interpolation of channel coefficients. The first step is common for both compared methods, as mentioned in Section 2. Pilot averaging is an optional step which is intended to reduce the adverse effect of noise on pilot estimates in low SNR conditions. By default, it is enabled and configured to use a frequency-time window the size of 13 by 9 resource elements. The final step performs 2D cubic interpolation independently for each subframe, preceded by generation of virtual pilots outside the subframe boundary.

Figures 9 and 10 show the results of SNR performance comparison between MLT and TIFA. As expected, both methods perform better in the AWGN scenario than in the fading channel scenario. It may be observed that, for all the considered SNR values and channel profiles, TIFA provides lower phase RMS error than the estimation method from MATLAB LTE Toolbox™. Error reduction is approximately 3% on average. The advantage of TIFA over MLT is especially visible for low SNR values. The same applies to symbol correlation represented by ρ_{IQ}. In the AWGN scenario, as SNR increases ρ_{IQ} approaches

1.0 value, which corresponds to a perfect match between equalized and original symbols. The average difference in ρ_{IQ} between TIFA and MLT is approximately 5–6%.

	AWGN		EPA5	
SNR	**MLT**	**TIFA**	**MLT**	**TIFA**
−5	1.43	1.38	1.47	1.44
0	1.01	0.95	1.22	1.19
5	0.56	0.54	0.87	0.83
10	0.30	0.30	0.59	0.58

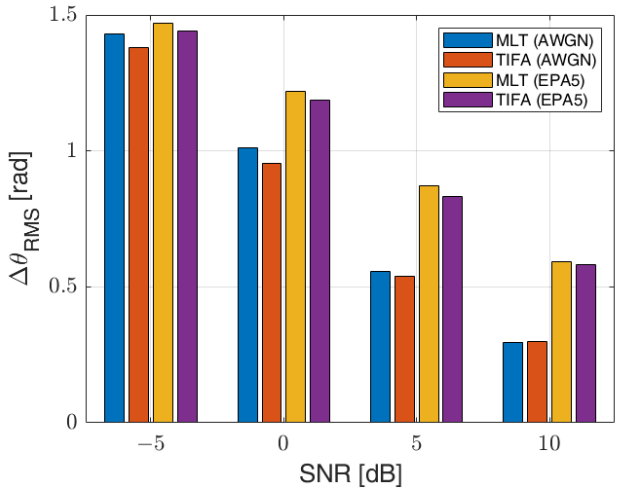

Figure 9. Phase RMS error for MLT and TIFA channel estimation methods in AWGN channel and fading (EPA5) channel.

	AWGN		EPA5	
SNR	**MLT**	**TIFA**	**MLT**	**TIFA**
−5	0.357	0.404	0.293	0.314
0	0.699	0.779	0.476	0.504
5	0.942	0.960	0.720	0.755
10	0.998	0.998	0.879	0.895

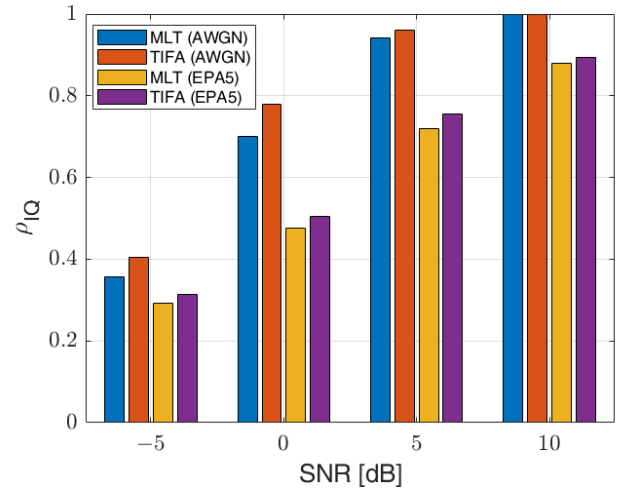

Figure 10. Symbol correlation coefficient for MLT and TIFA channel estimation methods in AWGN channel and fading (EPA5) channel.

In addition to channel estimation quality indicators, the percentage of successfully decoded information blocks, MIB-NB and SIB1-NB, was evaluated. The results are presented in Figure 11. For MIB-NB, the results for MLT and TIFA are very similar, except the case of the EPA profile with −5 dB SNR, where TIFA outperforms MLT by 4%. The difference between the two methods is more distinct in the case of SIB1-NB decoding. Especially for low SNR, a significant advantage of TIFA is observed. The number of decoded SIBs doubled when TIFA was applied to the EPA channel at −5 dB SNR. In general, the percentage of successfully decoded MIBs is higher than that of SIBs due to smaller transmission redundancy of the latter. For MIB-NB in standalone operation mode, 128 OFDM resource elements are used per one bit of transport block, while for SIB1-NB this ratio is approximately 99 resource elements per bit in the analyzed transmission scheme.

MIB-NB

	AWGN		EPA5	
SNR	**MLT**	**TIFA**	**MLT**	**TIFA**
−5	97.2%	97.2%	80.0%	84.1%
0	99.9%	99.9%	98.3%	98.2%
5	100.0%	100.0%	99.7%	99.6%
10	100.0%	100.0%	99.9%	99.9%

SIB1-NB

	AWGN		EPA5	
SNR	**MLT**	**TIFA**	**MLT**	**TIFA**
−5	76.1%	91.5%	26.6%	54.6%
0	98.6%	99.8%	90.2%	94.2%
5	99.8%	99.9%	97.9%	99.0%
10	100.0%	100.0%	99.5%	99.7%

Figure 11. Percentage of decoded MIB-NB ans SIB1-NB information blocks among trials with successful synchronization.

5.3. Comparison of Processing Time

To verify the low complexity of the proposed channel estimation method, the duration of MLT and TIFA processing was evaluated and compared. Since the first stage, i.e., LS pilot estimation, is the same for both methods, it was excluded from the time measurement. Moreover, the pilot averaging phase in the MLT method was excluded as well due to it being an optional step. Consequently, only the processing times required for the interpolation of channel coefficients were compared. MLT uses MATLAB's inbuilt *griddata* function to perform cubic interpolation. The source code of this function was customized so that all the unnecessary fragments, i.e., validation of input arguments and handling exceptions, could be removed to minimize the processing time.

In order to evaluate the processing time, *tic toc* stopwatch functions were used. They counted the total time required to interpolate channel coefficients for 128 consecutive NB-IoT frames. For each channel estimation method, 80 iterations were conducted using waveforms with different SNR values and channel profiles. The platform used for the processing was equipped with an i7-10700 CPU. Table 2 presents the minimum, maximum and mean value of all the processing times. The results show that the linear interpolation and averaging procedure proposed in TIFA is about seven times faster than cubic interpolation used in the MLT method.

Table 2. Duration of channel coefficient interpolation for consecutive 128 NB-IoT frames.

Method	Min	Max	Mean
MLT	547 ms	619 ms	563 ms
TIFA	69 ms	95 ms	74 ms

5.4. Comparison with Other Channel Estimation Methods

Most studies reported in the literature focus on improving the quality of channel estimation methods. The performance of these methods is typically evaluated using mean squared error (*MSE*) or bit error rate (BER) as functions of SNR. These indicators can be evaluated under the condition that the true values of channel coefficients and bits over time are known. Although it is not a problem for simulation research, this information is not available when capturing and analyzing live signals, as in this case. However, it is possible to obtain a rough estimate of *MSE*. The *MSE* of channel estimation is calculated as follows [34]:

$$MSE = \mathbb{E}\{(\mathbf{h} - \hat{\mathbf{h}})^*(\mathbf{h} - \hat{\mathbf{h}})\}, \tag{7}$$

where $\mathbf{h}$ and $\hat{\mathbf{h}}$ correspond, respectively, to the vectors of true and estimated channel coefficients, and * denotes the complex conjugate. Although the elements of $\mathbf{h}$ are not known, they can be estimated based on the restored values of transmitted resource elements:

$$\mathbf{h}' = \frac{\mathbf{y_i}}{\mathbf{x_i}}, \tag{8}$$

where $\mathbf{x_i}$ and $\mathbf{y_i}$ correspond to the vectors of true (restored) resource element values and received resource element values, respectively. The $\mathbf{h}'$ can be seen as an estimate of the channel coefficient, which is influenced by errors caused not only by the AWGN, but also by hardware-related factors such as phase noise, I/Q impairments, frequency offset, sampling offset, and others.

Table 3 presents the MSE values for MLT and TIFA methods in the fading channel. These values are similar to the values obtained for the conventional LS approach in simulation research, as shown in [6,14,16,18,20,22]. This shows that using a simplified channel coefficient population scheme does not negatively affect the overall SNR performance of the channel estimation procedure.

Table 3. Channel estimation MSE estimated for fading (EPA 5) channel.

SNR	MLT	TIFA
−5 dB	2.13	1.98
0 dB	0.71	0.63
5 dB	0.24	0.21
10 dB	0.07	0.06

6. Discussion

The results presented in the previous section show that the proposed downlink channel estimation method is well suited for application in the NB-IoT UE which requires low complexity due to its limitations on cost and power consumption. The initially considered method using linear interpolation in both time and frequency domains was further simplified so that frequency interpolation was substituted with frequency averaging. The modified method turned out to provide considerably higher estimation accuracy than the original one, especially for the AWGN channel at low SNR. When compared to the existing method, implemented in MATLAB LTE Toolbox™, the proposed solution offers several percent of improvement in terms of SNR performance. However, the major advantage of the described method is a several-fold reduction in computation time required for the interpolation of channel coefficients.

Although NB-IoT UEs have been available in the market for a few years, there is still a demand to reduce their power consumption in order to prolong their operational time. Along with power-saving features such as Discontinuous Reception (DRX), energy efficiency can be improved by developing less computationally intensive algorithms for physical layer processing, particularly in the receive chain. The method proposed in this paper provides a good balance between complexity and SNR performance. The combination of least squares estimation with linear interpolation and averaging results

in a very low computational burden while still providing comparable quality (MSE vs. SNR) compared to other LS-based methods. It should be noted that the complexity of the proposed solution is currently assessed solely by comparing processing times. The complete assessment of its advantages necessitates actual hardware implementation and a long-term analysis of power consumption.

It should be noted that the performance of any channel estimation method is dependent on the properties of the propagation environment, especially on the power delay profile which determines whether the channel is frequency-selective or not. 3GPP technical documents do not specify a typical profile for NB-IoT radio access channel. However, it may be assumed that for fixed UE located indoors, the channel response is generally short and changes less rapidly than in the vehicular case. Thus, assuming the pedestrian propagation model with low Doppler frequency shift is justified in the author's opinion. The same model was used to simulate the NB-IoT channel in [35]. It was proven that the proposed method is well suited for such a model. However, due to the variety of IoT applications, more challenging propagation conditions may occur, which requires further investigation.

Funding: This research received no external funding.

Institutional Review Board Statement: Not applicable.

Informed Consent Statement: Not applicable.

Data Availability Statement: The data presented in this study are available on request from the corresponding author. The data are not publicly available due to privacy.

Conflicts of Interest: The author declares no conflict of interest.

Abbreviations

The following abbreviations are used in this manuscript:

AWGN	Additive white Gaussian noise
EPA	Extended pedestrian A model
LS	Least squares
MIB-NB	Master Information Block for NB-IoT
MLT	MATLAB LTE Toolbox
NB-IoT	Narrowband Internet of Things
NPSS	Narrowband primary synchronization signal
NRS	Narrowband reference signal
NSSS	Narrowband secondary synchronization signal
OFDM	Orthogonal frequency division multiplexing
PRB	Physical resource block
QPSK	Quadrature phase-shift keying
RMSE	Root mean square error
SIB1-NB	System Information Block Type 1 for NB-IoT
SNR	Signal-to-noise ratio
TIFA	Time interpolation frequency averaging
TIFI	Time interpolation frequency interpolation
UE	User equipment

References

1. Chen, M.; Miao, Y.; Hao, Y.; Hwang, K. Narrow Band Internet of Things. *IEEE Access* **2017**, *5*, 20557–20577. [CrossRef]
2. Ratasuk, R.; Mangalvedhe, N.; Zhang, Y.; Robert, M.; Koskinen, J.P. Overview of narrowband IoT in LTE Rel-13. In Proceedings of the 2016 IEEE Conference on Standards for Communications and Networking (CSCN), Berlin, Germany, 31 October–2 November 2016; pp. 1–7.
3. Beyene, Y.D.; Jantti, R.; Ruttik, K.; Iraji, S. On the performance of narrow-band Internet of Things (NB-IoT). In Proceedings of the 2017 IEEE Wireless Communications and Networking Conference (WCNC), San Francisco, CA, USA, 19–22 March 2017; pp. 1–6.
4. Lin, D.D.; Pacheco, R.A.; Lim, T.J.; Hatzinakos, D. Joint estimation of channel response, frequency offset, and phase noise in OFDM. *IEEE Trans. Signal Process.* **2006**, *54*, 3542–3554.

5. Septier, F.; Delignon, Y.; Menhaj-Rivenq, A.; Garnier, C. OFDM channel estimation in the presence of phase noise and frequency offset by particle filtering. In Proceedings of the 2007 IEEE International Conference on Acoustics, Speech and Signal Processing-ICASSP'07, Honolulu, HI, USA, 15–20 April 2007; Volume 3, pp. III-289–III-292.
6. Tao, J.; Wu, J.; Xiao, C. Estimation of channel transfer function and carrier frequency offset for OFDM systems with phase noise. *IEEE Trans. Veh. Technol.* **2009**, *58*, 4380–4387.
7. Zhang, P.; He, J.; Dong, J.; Sha, L. Joint Frequency Offset and Channel Estimation for NB-IoT Systems. *J. Netw. Netw. Appl.* **2022**, *2*, 61–67. [CrossRef]
8. Kanj, M.; Savaux, V.; Le Guen, M. A tutorial on NB-IoT physical layer design. *IEEE Commun. Surv. Tutor.* **2020**, *22*, 2408–2446. [CrossRef]
9. Akpakwu, G.A.; Silva, B.J.; Hancke, G.P.; Abu-Mahfouz, A.M. A survey on 5G networks for the Internet of Things: Communication technologies and challenges. *IEEE Access* **2017**, *6*, 3619–3647. [CrossRef]
10. Fattah, H. *5G LTE Narrowband Internet of Things (NB-IoT)*; CRC Press: Boca Raton, FL, USA, 2018.
11. Wang, Y.P.E.; Lin, X.; Adhikary, A.; Grovlen, A.; Sui, Y.; Blankenship, Y.; Bergman, J.; Razaghi, H.S. A primer on 3GPP narrowband Internet of Things. *IEEE Commun. Mag.* **2017**, *55*, 117–123. [CrossRef]
12. 3GPP. LTE; Evolved Universal Terrestrial Radio Access (E-UTRA); Physical channels and modulation. Technical Specification (TS) 36.211, 3rd Generation Partnership Project (3GPP), 2020. Version 14.14.0. Available online: https://www.etsi.org/deliver/etsi_ts/136200_136299/136211/14.14.00_60/ts_136211v141400p.pdf (accessed on 17 October 2023).
13. Zhang, S.; Zeng, S.; Ye, F.; Tang, R.; Wu, P.; Xia, M. An efficient downlink receiver design for NB-IoT. In Proceedings of the 2020 IEEE Wireless Communications and Networking Conference (WCNC), Virtual Conference, 25–28 May 2020; pp. 1–6.
14. Van De Beek, J.J.; Edfors, O.; Sandell, M.; Wilson, S.K.; Borjesson, P.O. On channel estimation in OFDM systems. In Proceedings of the 1995 IEEE 45th Vehicular Technology Conference. Countdown to the Wireless Twenty-First Century, Chicago, IL, USA, 25–28 July 1995; Volume 2, pp. 815–819.
15. Noh, M.; Lee, Y.; Park, H. Low complexity LMMSE channel estimation for OFDM. *IEE Proc.-Commun.* **2006**, *153*, 645–650. [CrossRef]
16. Edfors, O.; Sandell, M.; Van de Beek, J.J.; Wilson, S.K.; Borjesson, P.O. OFDM channel estimation by singular value decomposition. *IEEE Trans. Commun.* **1998**, *46*, 931–939. [CrossRef]
17. Morelli, M.; Mengali, U. A comparison of pilot-aided channel estimation methods for OFDM systems. *IEEE Trans. Signal Process.* **2001**, *49*, 3065–3073. [CrossRef]
18. Rana, M.M. Channel estimation techniques and LTE Terminal implementation challenges. In Proceedings of the 2010 13th International Conference on Computer and Information Technology (ICCIT), Dhaka, Bangladesh, 23–25 December 2010; pp. 545–549.
19. Simko, M.; Wu, D.; Mehlführer, C.; Eilert, J.; Liu, D. Implementation aspects of channel estimation for 3GPP LTE terminals. In Proceedings of the 17th European Wireless 2011—Sustainable Wireless Technologies, Vienna, Austria, 27–29 April 2011; pp. 1–5.
20. Khlifi, A.; Bouallegue, R. Performance analysis of LS and LMMSE channel estimation techniques for LTE downlink systems. *arXiv* **2011**, arXiv:1111.1666.
21. Song, H.; Li, X.; Yu, Z. A complexity reduction approach for LTE downlink channel estimation. In Proceedings of the 2011 International Conference on Internet Technology and Applications, Wuhan, China, 16–18 August 2011; pp. 1–4.
22. Wang, S.; Hu, C.; Peng, T.; Wang, W. A low complexity channel estimation approach of LTE downlink system. In Proceedings of the 2012 IEEE 14th International Conference on Communication Technology, Chengdu, China, 9–11 November 2012; pp. 143–147.
23. Rusek, F.; Hu, S. Sequential channel estimation in the presence of random phase noise in NB-IoT systems. In Proceedings of the 2017 IEEE 28th Annual International Symposium on Personal, Indoor, and Mobile Radio Communications (PIMRC), Montreal, QC, Canada, 8–13 October 2017; pp. 1–5.
24. Ali, M.S.; Jewel, M.K.H.; Lin, F. An efficient channel estimation technique in NB-IoT systems. In Proceedings of the 2018 IEEE International Conference on Integrated Circuits, Technologies and Applications (ICTA), Beijing, China, 21–23 November 2018; pp. 22–23.
25. Jewel, M.K.H.; Zakariyya, R.S.; Famoriji, O.J.; Ali, M.S.; Lin, F. A low complexity channel estimation technique for NB-IoT downlink system. In Proceedings of the 2019 IEEE MTT-S International Wireless Symposium (IWS), Guangzhou, China, 19–22 May 2019; pp. 1–3.
26. Jewel, M.K.H.; Zakariyya, R.S.; Lin, F. On channel estimation in LTE-based downlink narrowband Internet of Things systems. *Electronics* **2021**, *10*, 1246. [CrossRef]
27. Jewel, M.K.H.; Zakariyya, R.S.; Lin, F. A Pilot-based Hybrid and Reduced Complexity Channel Estimation Method for Downlink NB-IoT Systems. In Proceedings of the 2020 IEEE MTT-S International Wireless Symposium (IWS), Shanghai, China, 20–23 September 2020; pp. 1–3.
28. 3GPP. LTE; Evolved Universal Terrestrial Radio Access (E-UTRA); User Equipment (UE) radio transmission and reception. Technical Specification (TS) 36.101, 3rd Generation Partnership Project (3GPP), 2017. Version 14.3.0. Available online: https://www.etsi.org/deliver/etsi_ts/136100_136199/136101/14.03.00_60/ts_136101v140300p.pdf (accessed on 17 October 2023).
29. Staniec, K.; Kucharzak, M.; Jóskiewicz, Z.; Chowański, B. Measurement-Based Investigations of the NB-IoT Downlink Performance in Fading Channels. *IEEE Wirel. Commun. Lett.* **2021**, *10*, 1780–1784. [CrossRef]

30. Schlienz, J.; Raddino, D. *Narrowband Internet of Things (White Paper)*; Rohde Schwarz: Tokyo, Japan, 2016; pp. 1–42. Available online: https://www.rohde-schwarz.com/us/applications/narrowband-internet-of-things-white-paper_230854-314242.html (accessed on 30 September 2023).
31. Rohde & Schwarz CMW500 Wideband Radio Communication Tester. Available online: https://www.rohde-schwarz.com/us/products/test-and-measurement/wireless-tester-network-emulator/rs-cmw500-wideband-radio-communication-tester_63493-10844.html (accessed on 30 September 2023).
32. Chettri, L.; Bera, R.; Barauh, J.K. Performance Analysis of 3GPP NB-IoT Downlink System towards 5G Machine Type Communication (5G-MTC). *J. Commun.* **2021**, *16*, 355–362. [CrossRef]
33. MathWorks Documentation NB-IoT Cell Search and MIB Recovery. Available online: https://www.mathworks.com/help/lte/ug/nb-iot-cell-search-and-mib-recovery.html (accessed on 30 September 2023).
34. Andres-Maldonado, P.; Ameigeiras, P.; Prados-Garzon, J.; Navarro-Ortiz, J.; Lopez-Soler, J.M. An analytical performance evaluation framework for NB-IoT. *IEEE Internet Things J.* **2019**, *6*, 7232–7240. [CrossRef]
35. Won, J.W.; Ahn, J.M. NB-IoT Downlink Channel Estimation. In Proceedings of the 2020 International Conference on Information and Communication Technology Convergence (ICTC), Jeju, Korea, 21–23 October 2020; pp. 1739–1741.